

Plastic and Reconstructive Surgery, Successful treatment with vascularized lymph node transfer and adipose stem cells in a mouse hindlimb lymphedema model

1

2

3 Adipose-Derived Stem Cells and Vascularized Lymph Node
4 Transfers Successfully Treat Mouse Hindlimb Secondary
5 Lymphedema by Early Re-connection of the Lymphatic System and
6 Lymphangiogenesis

7

8

9 Kenji Hayashida^{1,2,3} , Shuhei Yoshida¹ , Hiroshi Yoshimoto¹ , Masaki
10 Fujioka² , Hiroto Saijo² , Kiyoshi Migita³ , Misato Kumaya⁴ , Sadanori
11 Akita^{1*}

12

13 1: Department of Plastic and Reconstructive Surgery, Nagasaki
14 University Graduate School of Biomedical Sciences

15 2: Department of Plastic and Reconstructive Surgery, National
16 Nagasaki Medical Center

17 3: Department of Molecular Immunology, Nagasaki University
18 Graduate School of Biomedical Sciences

Plastic and Reconstructive Surgery, Successful treatment with vascularized lymph node transfer and adipose stem cells in a mouse hindlimb lymphedema model

19 4: Oita University

20

21

22

23 *Correspondence should be addressed to:

24 Sadanori Akita

25 Tel.: +81 95 819 7327

26 Fax: +81 95 819 7330

27 E-mail: akitas@hf.rim.or.jp

28

29 Department of Plastic and Reconstructive Surgery

30 Nagasaki University Hospital

31 1-7-1 Sakamoto, Nagasaki, 8528501, Japan

32

33 There is no financial source in this manuscript

34

35

Plastic and Reconstructive Surgery, Successful treatment with vascularized lymph node transfer and adipose stem cells in a mouse hindlimb lymphedema model

36 Running head: Successful treatment with vascularized lymph node

37 transfer and adipose stem cells in a mouse hindlimb lymphedema

38 model

39

40

Plastic and Reconstructive Surgery, Successful treatment with vascularized lymph node transfer and adipose stem cells in a mouse hindlimb lymphedema model

41 **Abstract**

42 **Background:** Secondary lymphedema is often observed in post-
43 malignancy treatment of the breast and the gynecologic organs, but
44 effective therapies have not been established in chronic cases even
45 with advanced physiological surgeries. Currently, reconstructive
46 surgery with novel approaches has been attempted.

47 **Methods:** The hindlimbs of 10-week-old male C57BL/6J mice, after 30
48 Gy X-ray radiation, surgical lymph node dissection, and 5-mm gap
49 creation, were divided into 4 groups, with vascularized lymph node
50 transfer (VLNT) abdominal flap, and 1.0×10^4 adipose-derived stem
51 cells (ADSC). Lymphatic flow assessment, a water-displacement
52 plethysmometer paw volumetry test, tissue quantification of
53 lymphatic vessels, and functional analysis of lymphatic vessels and
54 nodes were performed.

55 **Results:** Photo Dynamic Eye (PDE) images using, indocyanine green
56 fluorescence, demonstrated immediate staining in subiliac lymph
57 nodes, and linear pattern imaging of the proximal region was
58 observed in the combined treatment of ADSC and VLNT. Both
59 percent improvement and percent deterioration in the combined
60 treatment of ADSC and VLNT were significantly better than in other
61 treatments ($p < 0.05$). The numbers of lymphatic vessels with LYVE-1
62 immunoreactivity significantly increased when treated with ADSCs
63 ($P < 0.05$) and B16 melanoma cells were metastasized in groups
64 treated with VLNTs by day 28.

65 **Conclusion:** ADSCs increase the number of lymphatic vessels and
66 VLNTs induce the lymphatic flow drainage to the circulatory system.
67 Combined ADSC and VLNT treatment in a secondary lymphedema
68 may effectively decrease edema volume and lymphatic function by
69 lymphangiogenesis and the lymphatic to venous circulation route.

70
71
72
73
74
75
76

77 **INTRODUCTION**

78 Lymphedema is caused by, and consists of, chronic inflammation
79 and the impairment of the lymphatic systems of collection, drainage,
80 and circulation of interstitial protein-rich fluid.

81 Among lymphedema, secondary lymphedema is acquired as a result
82 of trauma, surgery, radiotherapy, infection, or a combination of these,
83 and it occurs more frequently than primary lymphedema. Cancer
84 therapy with radical surgical lymph node dissection and
85 radiotherapy may result in severe impairment of the lymphatic
86 systems, and radiation causes tissue fibrosis and further destruction
87 of the lympho-reticuloendothelial system.

88 Treatment of lymphedema is still challenging even with surgeries
89 that are performed in severe and refractory cases as well as
90 conservative therapies (1).

91 Lymphovenous anastomoses (LVA), which create a bypass for the
92 lymphatic fluid return to venous systems and require refined surgical
93 skills, may be effective in early-stage lymphedema, but not in later-
94 stage or advanced-stage lymphedemas (2,3), possibly due to the loss
95 of the lymphatic vessels' ability to transfer lymph fluid in later stages.

Plastic and Reconstructive Surgery, Successful treatment with vascularized lymph node transfer and adipose stem cells in a mouse hindlimb lymphedema model

96 Another physiological surgical option is a vascularized lymph node
97 transfer (VLNT), and in this method, vascularized lymph nodes are
98 transferred into areas where lymph nodes have been dissected for
99 cancer treatment or into distal regions of lymphedematous distal
100 tissue, such as limbs, to restore lymphatic drainage function. Becker
101 et al. (4) reported, for the first time, post-mastectomy clinical cases of
102 VLNT with promising results and has been followed by other such
103 cases in upper limbs (5, 6) and lower limbs (7). Despite promising
104 clinical results, widespread application of VLNT is not yet underway.

105 Aside from such transplanting and reconstructive surgeries,
106 pharmacologic agents like VEGF-C are potently lymphangiogenic (8),
107 which was elucidated in an overexpression transgenic model
108 targeting the skin and lymphatic endothelial cells, and the signal of
109 VEGF-C was transduced by VEGFR-3, and shown to be involved in
110 growth, survival, and migration (9).

111 Adipose-derived stem cells, ADSCs, are candidates for a novel
112 therapeutic modality because of their multi-differential capacities
113 and marked enhancement of lymphatic endothelial cell (LEC)

Plastic and Reconstructive Surgery, Successful treatment with vascularized lymph node transfer and adipose stem cells in a mouse hindlimb lymphedema model

114 proliferation in vitro, as well as the tube formation, migration, and
115 expression of lymphangiogenic factors and the regulation of Prox-1
116 and VEGFR-3 expression (10). ADSCs successfully induced
117 lymphangiogenesis (11) and VEGF-C in a hydrogel with ADSCs
118 demonstrated decreased dermal edema and enhanced lymphatic
119 vessel regeneration (12).

120

121 We investigated both VLNT and ADSCs in a mouse hindlimb
122 chronic secondary lymphedema model, which was created by a single
123 dose of 30 Gy of radiation, surgical removal of complete lymph nodes
124 and lymphatic systems in situ. The mice underwent transfer of an
125 abdominal flap, plus or minus vascularized lymph nodes, plus or
126 minus ADSCs. This may be more consistent with and reflects clinical
127 secondary lymphedema, as radiation therapy and surgery are often
128 used as an adjuvant or mainstay of the treatment (13-17). Our
129 findings may provide information about the pathogenesis of
130 secondary lymphedema and the possible implications of both adipose-

Plastic and Reconstructive Surgery, Successful treatment with vascularized lymph node transfer and adipose stem cells in a mouse hindlimb lymphedema model

131 derived stem cell therapy and VLNT as potential therapeutic

132 modalities.

133

134 **MATERIALS AND METHODS**

135 **Secondary lymphedema mouse model**

136 Lymphedema was established in the left hind limbs of 10-week-old
137 male C57BL/6J mice (Charles River Laboratories Japan, Inc.). All
138 studies were approved by the Institutional Animal Care and Use
139 Committee (IACUC) of Nagasaki University, #1007150867-4.

140 In order to establish a lymphedema model, the mice were subjected
141 to X-ray radiation in the left inguinal region at 30 Gy in a single dose
142 7 days prior to the surgery. After radiation, mice were then subjected
143 to circumferential incision in the inguinal region of the muscle layer.
144 Under a microscope, the popliteal lymph nodes were removed, and
145 the superficial collecting lymph vessels were cut and cauterized, and
146 the 5-mm wide gap was left open (Figure 1)(Table 1)(11).

147

148 **Vascularized lymph node transfer (VLNT) surgery**

149 After simultaneously establishing a lymphedema mouse model, an
150 ipsilateral left abdomino-cutaneous flap based on the left superficial
151 inferior epigastric artery, containing subiliac lymph nodes, was

152 meticulously elevated en bloc using dissecting scissors under a
153 microscope (Figure 2)(Figure 3). The elevated flap contained skin,
154 subcutaneous fat, and subiliac lymph nodes. The flap was transferred
155 and inset into the 5-mm wide inguinal defects to set the vascularized
156 subiliac lymph nodes onto the site where popliteal lymph nodes had
157 been removed from. Skin at donor and recipient sites was directly
158 closed.

159

160

161 **Preparation of adipose-derived stem cells**

162 Adipose-derived stem cells (ADSCs) were isolated as previously
163 described (11). ADSCs were harvested from the adipose tissue of 10
164 individual animals of the same species of 10-week-old male C57BL/6J
165 mice.

166 An average of 2.89 ± 0.5 g of adipose tissue was harvested from the
167 intra-abdominal and inguinal regions, taking care to identify and
168 remove lymph nodes. Harvested adipose tissue was minced into
169 pieces smaller than 3 mm. ADSCs from the first to three passages

170 were used for cell transplantation. The ADSCs were counted with a
171 Beckman Coulter Z1 (Beckman Coulter, Inc., Japan).

172

173 **Grouping of the experimental animals**

174 The mice prepared for lymphedema were divided into 4 groups.

175 Both no VLNT and VLNT groups were subdivided into another two
176 groups according to whether ADSCs were transplanted or not.

177 In no VLNT groups, each mouse had the subiliac lymph nodes
178 carefully removed from the flap under a microscope, and then the
179 flap with no lymph nodes was transferred.

180 In the ADSC groups, each mouse had 1×10^4 ADSCs injected with 0.3
181 ml of phosphate-buffered saline (PBS). Each solution was injected
182 subcutaneously into the entire flap, proximal (to the flap) limbs, and
183 distal (to the flap) limbs equally, just after surgery, with a 30G
184 needle. In no ADSC groups, the mock injection of PBS solutions was
185 performed in a similar manner.

186

Plastic and Reconstructive Surgery, Successful treatment with vascularized lymph node transfer and adipose stem cells in a mouse hindlimb lymphedema model

187 Group 1 (control), no VLNT group, n = 5, was injected with only 0.3
188 ml PBS.

189 Group 2, VLNT group, n = 5, was injected with only 0.3 ml PBS.

190 Group 3, no VLNT group, n = 5, was injected with 1.0×10^4 ADSCs
191 with 0.3 ml PBS.

192 Group 4, VLNT group, n = 5, was injected with 1.0×10^4 ADSCs with
193 0.3 ml PBS.

194

195 **Assessment using a near-infrared video camera system (PDE)**

196 Lymphatic flow assessment using a fluorescence near-infrared
197 video camera system, Photodynamic Eye® (Pde-neo®, Hamamatsu,
198 Japan), was performed with the intradermal injection of Indocyanine
199 Green (ICG), Diagnogreen® (Daiichi Sankyo Company, Ltd., Tokyo,
200 Japan). 0.1 mg of ICG was injected into the left paw. After 5 minutes,
201 the observation was carried out.

202

203 **Measurement of hind paw edema volume**

Plastic and Reconstructive Surgery, Successful treatment with vascularized lymph node transfer and adipose stem cells in a mouse hindlimb lymphedema model

204 The left hind paw volume was measured with a water-displacement
205 plethysmometer (MK-101 CMP; Muromachi Kikai Co., Ltd., Japan).
206 Quantitative measurements at the same site (the musculotendinous
207 junction of the gastrocnemius muscle) were performed under
208 anesthesia before the surgery, 2 days after surgery, and 14 days after
209 surgery, by blinded evaluators devoid of knowing the attributing
210 groups. Measurements of the left hind paw volume were repeated 3
211 times at each time point, and the mean values were statistically
212 analyzed. The effectiveness of treatment improvement were
213 quantitatively calculated using the mean percent Δ value normalized
214 by each volume at 2 days, on which swelling was most severe. Each
215 Δ value was calculated by subtracting the volume at 2 days from the
216 volume at 14 days, in which the effect is considered most profound.
217 Similarly, the percent deterioration was quantitatively calculated by
218 the mean percent Δ value normalized by each pre-surgery volume.
219 Each Δ value was calculated by subtracting the pre-surgery volume
220 from the volume at day 14. The study design is summarized in Table
221 1.

Plastic and Reconstructive Surgery, Successful treatment with vascularized lymph node transfer and adipose stem cells in a mouse hindlimb lymphedema model

222

223 **Histological examination**

224 After the evaluation of the dynamic changes of PDE, the transferred
225 flaps, including their vascularized lymph nodes, were carefully
226 harvested for tissue sampling.

227

228 **LYVE-1 immunoreactivity**

229 The tissue was fixed immediately with 4% paraformaldehyde and
230 embedded in paraffin. The embedded specimens were sectioned (5
231 μm) along the longitudinal axis of the flaps, immersed in (pure)
232 xylene for 20 minutes each, and then sequentially immersed in 80%,
233 90%, 95%, and 100% ethanol for 5 minutes for deparaffinization.
234 After antigen retrieval with microwave treatment in citrate buffer at
235 120 °C for 10 min, sections were pre-incubated with 10% normal goat
236 serum. After immersion in 0.3% H_2O_2 , tissues were incubated
237 overnight at 4 °C with anti-LYVE-1 antibodies, a lymphatic vessel
238 marker (Mouse LYVE-1 Antibody Polyclonal Goat IgG, AF 2125, R&
239 D Systems), at a 1:100 dilution. The slides were subsequently simple

Plastic and Reconstructive Surgery, Successful treatment with vascularized lymph node transfer and adipose stem cells in a mouse hindlimb lymphedema model

240 stained with goat MAX-PO, and then visualized with the
241 chromogenic substrate diaminobenzidine (DAB).
242 Sections stained with LYVE-1 were scanned at low magnification
243 (20×) to select areas containing the most lymphatic vessels (hot spots).
244 Five hot spots within each section were measured at high
245 magnification, and the lymphatic vessel density was calculated as the
246 mean number of lymphatic vessels in hot spots per field.

247

248 **VEGF-C and VEGF-R3 immunoreactivity**

249 After deparaffinization and antigen retrieval, tissues were incubated
250 overnight at 4 °C with anti-VEGF-C polyclonal antibodies (Rabbit
251 polyclonal antibody to VEGF-C, GTX113574, Genetex) at 1:100
252 dilution or anti-VEGF receptor 3 monoclonal antibodies (Rabbit
253 polyclonal antibody to VEGF Receptor 3, ab27278, Abcam) at 1:100
254 dilution. The slides were subsequently labeled with Biotin (LSAB2),
255 and then visualized with DAB. Sections stained with VEGF-C, or
256 VEGF-R3, were evaluated at high magnification.

257

258 **Analysis of lymphatic vessel and lymph node function**

259 To determine whether the lymphatic fluid is passing through the
260 transferred lymph nodes or not in such conditions, 5×10^5 B16 mouse
261 melanoma cells (JCRB0202, JCRB, Japan) were transplanted
262 subcutaneously into the left paw at the same time of VLNT alone,
263 VLNT plus /ADSC minus group (similar to Group 2: n=6) and VLNT
264 and ADSCs, VLNT plus /ADSC plus group (similar to Group 4: n=6).
265 The lymph nodes and metastatic skin tumors were harvested from
266 the mice, for histology, at 21 days (VLNT plus /ADSC minus group:
267 n=3 and VLNT plus /ADSC ~~minus~~ **plus** group: n=3) and 28 days
268 (VLNT plus /ADSC minus group: n=3) after transplantation. The
269 tissues were evaluated using Melan-A immunoreactivity. After
270 immersion in 1.0% H₂O₂, the tissues were incubated overnight at
271 4 °C with mouse monoclonal antibodies (DT101 + BC199) to Melan-A
272 (ab731, Abcam) at a 1:100 dilution. The slides were subsequently
273 labeled with anti-mouse immunoglobulins/HRP, and then visualized
274 with amino-ethylcarbazole (AEC). Melan-A positive cells were
275 determined for each section.

Plastic and Reconstructive Surgery, Successful treatment with vascularized lymph node transfer and adipose stem cells in a mouse hindlimb lymphedema model

276

277

278 **Statistical analysis**

279 All statistical analyses were performed using Statview version 5 for
280 Windows (SAS Institute Inc., Cary NC).

281 An overall difference between the groups was determined by one-way
282 ANOVA. Post hoc multiple comparisons were made by using a Tukey-
283 Kramer all-pairwise-comparison test for parametric analysis. The
284 values are expressed as means \pm standard deviation (SD) and p-
285 values less than 0.05 were considered significant.

286 Animals are inbred, handling animals, surgical and management
287 procedures are uniformly established. According to this method, the
288 experiment should be of an appropriate size if the error degrees of
289 freedom in analysis of variance (ANOVA) area somewhere 10 and 20
290 (18, 19).

291

292 The equation is calculated as below;

293

Plastic and Reconstructive Surgery, Successful treatment with vascularized lymph node transfer and adipose stem cells in a mouse hindlimb lymphedema model

294 $X = N \cdot T \cdot B + 1$

295

296 N= total number of animals

297 T=the number of treatment

298 B=the number of groups

299

300 In this manuscript, N=20, T=4 and B=4

301

302 Therefore, $X = 20 \cdot 4 \cdot 4 + 1 = 13$

303

304 This number “13” is sought to be considered appropriate for the
305 experimental design.

306

307 **RESULTS**

308 Apparent swelling peaked macroscopically at 2 days after surgery.

309 The appearances of hind limbs varied at 14 days, at which treatment
310 was stabilized (Figure 4-7).

311

Plastic and Reconstructive Surgery, Successful treatment with vascularized lymph node transfer and adipose stem cells in a mouse hindlimb lymphedema model

312 **PDE images**

313 ***PDE images of normal mouse hindlimbs***

314 Immediately after the injection of ICG to the paw, a bright spot was
315 seen on the foot. Within 5 minutes, lymphatic flow was visualized as
316 bright ICG fluorescence reaching the popliteal and subiliac lymph
317 nodes in prone and supine positions.

318

319 ***Group 1***

320 The features in the fluorescent imaging seemed to be spotted or
321 uniform. Fluorescent imaging toward the proximal trunk was not
322 observed in the irradiated region and thus the lymphedema was
323 lasting, which indicates no lymph flow as deep as can be observed
324 with the PDE. No fluorescent staining was present in the flaps
325 (Figure 8).

326

327 ***Group 2***

328 Fluorescent imaging toward the proximal trunks was not observed
329 in the irradiated region. However, in the transferred flap, the

Plastic and Reconstructive Surgery, Successful treatment with vascularized lymph node transfer and adipose stem cells in a mouse hindlimb lymphedema model

330 superficial inferior epigastric vein was detected by ICG staining
331 through the transferred lymph nodes. The flap was gradually stained
332 with mild lymph flows and the ICG passed through the efferent
333 lymphatic vessels into the venous system (Figure 9).

334

335 ***Group 3***

336 Small linear fluorescent imaging was observed in the proximal
337 region of the flap, which was supposed to restore superficial
338 collecting lymph vessels running along the ischiatic vein. Staining
339 was not observed within the flap (Figure 10).

340

341 ***Group 4***

342 Through the transferred subiliac lymph nodes, the flap was stained
343 immediately. The lymph node flap shunted lymphatic fluid from the
344 recipient bed, via lymph nodes, into the flap's pedicle vein. Linear
345 fluorescent imaging was also observed in the proximal region of the
346 flap as in Group 3 (Figure 11).

347

348 **Volumetric analysis**

349 The ranges of values of each group at 14 days after surgery were
350 0.294 to 0.480, 0.284 to 0.453, 0.312 to 0.438, and 0.241 to 0.265 ml in
351 Group 1, Group 2, Group 3 and Group 4, respectively.

352 The ranges of values of each group at 2 days after surgery were 0.317
353 to 0.513, 0.307 to 0.502, 0.343 to 0.548, and 0.370 to 0.539 ml in
354 Group 1, Group 2, Group 3 and Group 4, respectively.

355 The ranges of values of each group at pre-surgery were 0.109 to 0.149,
356 0.114 to 0.142, 0.119 to 0.153, and 0.102 and 0.145 ml in Group 1,
357 Group 2, Group 3 and Group 4, respectively.

358 The hind paw volume of Group 4 was significantly lower than in the
359 other groups at 14 days after surgery ($p < 0.05$) (Figure 12). The
360 percentage of improved difference was 10.0 ± 3.7 (range: 6.4 to 15.0),
361 7.9 ± 3.8 (range: 4.3 to 14.3), 13.0 ± 5.0 (range: 7.6 to 20.1), and $46.0 \pm$
362 7.0 (range: 34.0 to 50.9) in Group 1, Group 2, Group 3, and Group 4,
363 respectively, in between 2 days and 14 days after surgery. The ratio

Plastic and Reconstructive Surgery, Successful treatment with vascularized lymph node transfer and adipose stem cells in a mouse hindlimb lymphedema model

364 was significantly improved in Group 4 compared with other groups
365 ($p < 0.05$) (Figure 13).

366 The percentage of deterioration difference in each group was $198.2 \pm$
367 51.9 (range: 150.4 to 272.9), 186.2 ± 50.6 (range: 109.7 to 234.1),
368 199.7 ± 45.2 (range: 144.7 to 258.8), and 92.9 ± 36.8 (range: 68.8 to
369 154.5) in Group 1, Group 2, Group 3, and Group 4, respectively. The
370 volumetric deterioration significantly recovered in Group 4 compared
371 with other groups ($p < 0.05$) (Figure 14).

372

373 **Histological analysis**

374 There were no signs of transferred lymph node ischemia or necrosis
375 in both Group 2 and Group 4. Lymphatic vessels detected with
376 LYVE-1 immunoreactivity were seen around the transferred lymph
377 nodes.

378

379 **The number of lymphatic vessels with LYVE-1 immunoreactivity**

380 The numbers of LYVE-1-positive lymphatic vessels were 7.4 ± 0.9
381 (range: 6.4 to 8.6), 8.0 ± 0.6 (range: 7.4 to 8.6), 11.7 ± 0.4 (range: 11.2

382 to 12.4), and 11.5 ± 1.4 (range: 9.2 to 12.6) per field in Group 1, Group
383 2, Group 3, and Group 4, respectively. The numbers of lymphatic
384 vessels in Group 3 and Group 4 were significantly increased
385 compared with those in Group 1 and Group 2 (Figure 15) ($p < 0.05$).

386

387 **VEGF-C and VEGF-R3 immunoreactivity**

388 There were no VEGF-C or VEGF-R3 expressing cells in the
389 lymphatic vessels of any of the groups.

390

391 **Analysis of lymphatic transport capacity and function**

392 At 21 days after melanoma cell transplantation, only one of three
393 mice in VLNT plus /ADSC minus group developed lymph node
394 metastasis. In contrast, all mice in VLNT plus /ADSC plus group
395 (three of three mice) developed lymph node metastases. In addition,
396 there were metastatic skin tumors on the trunks of the mice in VLNT
397 plus /ADSC plus group only (Figure 16, 17).

398 All Group 4 mice died of tumor progression by day 25.

Plastic and Reconstructive Surgery, Successful treatment with vascularized lymph node transfer and adipose stem cells in a mouse hindlimb lymphedema model

399 By day 28, all mice in Group 2 (three of three mice) developed gross
400 lymph node metastases and in-transit metastases in their flaps.
401 The transferred lymph nodes were able to trap metastatic tumor cells
402 by forming new lymphatic vessels. Mice in Group 4 developed lymph
403 node metastases more quickly than those in Group 2. These findings
404 suggested that recanalization and reanastomoses of the lymphatic
405 vessels between the recipient and the transferred lymph node
406 occurred, as well as lymphangiogenesis, and efferent lymphatic fluid
407 was routed through the transferred lymph nodes and superficial
408 collecting lymph vessels (Figure 18, 19).

409 **Discussion**

410 In this experiment, PDE fluorescent imaging clearly depicted the
411 vascularized lymph node groups. In VLNT plus / ADSCs minus, the
412 superficial inferior epigastric vein was detected through the
413 transferred lymph nodes, and this may contribute to decreasing the
414 lymphedema, whereas in mice with VLNT plus and ADSCs plus, the
415 subiliac lymph nodes in the flap were stained immediately, then the
416 lymph node flap re-connected lymphatic fluid from the recipient bed,
417 via lymph nodes, into the flap's pedicle vessels and linear fluorescent
418 imaging was also observed in the proximal region of the flap. In this
419 experiment, the gap difference was 5 mm and the abdominal flap, in
420 fact a bit bigger than 5 mm in width as it shrinks after elevation, are
421 tested in this experiment. Regardless of VLNT minus and ADSCs
422 minus, group 1, either VLNT plus and ADSCS minus, group, 2 or
423 VLNT minus and ADSCs plus, group 3, failed the effective recovery
424 of lymph edema.

425 A relatively smaller dose of ADSCs, at 1.0×10^4 cells, successfully
426 demonstrated linear fluorescent imaging in the proximal region of

Plastic and Reconstructive Surgery, Successful treatment with vascularized lymph node transfer and adipose stem cells in a mouse hindlimb lymphedema model

427 the flap, which was supposed to restore superficial collecting lymph
428 vessels running along the ischiatic vein in mice with ADSCs plus and
429 VLNT minus. This finding is consistent with our previous data (11),
430 even though this current model is different in the manner in which
431 the vascularized flap was inserted.

432 Measurements of paw volume, represented in Figure 12,
433 quantitative measurements at the same site (the musculotendinous
434 junction of the gastrocnemius muscle), which seem much easier, more
435 repeatable, and more precise than circumferential measurements
436 (11), were determined by a water-displacement plethysmometer,
437 which can be compared with the angiotensin II type 1 receptor
438 adjuvant-induced arthritis rat model (20). It is dependent on the time
439 course of “edema” of this model. After establishing the animal model
440 by radiation, removal, flap or cell injection, the degree of “edema” is
441 peaking at day 2 and gradually the degree decreases by day 14,
442 where the “edema” reaches within the “plateau”. Thus, both day 2
443 and day 14 are chosen for analysis in this experiment. This animal
444 model is similarly confirmed in our previous study (11). In prevention

Plastic and Reconstructive Surgery, Successful treatment with vascularized lymph node transfer and adipose stem cells in a mouse hindlimb lymphedema model

445 of lymphedematous mouse hindlimb model with non-vascularized
446 lymph node transplantation (21), demonstrated the effects of VLNT,
447 ADSC, and their combination, and only the combination of VLNT and
448 ADSCs significantly improved the edema (close to 50%). Furthermore,
449 the percent deterioration in VLNT plus / ADSCs plus group is less
450 than 2-fold, while the other groups demonstrated around 10%
451 improvement and deteriorations approximately in the order of 3-fold.

452 Both VEGF-C and VEGFR3 immunoreactivity were not observed. In
453 the previous model, both VEGF-C and VEGFR3 were dose-
454 dependently increased from 1.0×10^4 , 1.0×10^5 to 1.0×10^6 cells in
455 the similar, but no vascularized flap inserted limb model (11). This
456 model is very different in terms of the local expression of VEGF-C
457 and VEGFR3, because VEGF-C/VEGFR3 are negatively regulated by
458 the action of fibroblast growth factors (FGFs) in an autocrine manner
459 as the inhibition of FGFR signaling in mouse mammary carcinoma
460 and rat glioma cancer cells suppresses VEGF-C expression in a COX-
461 2 (cyclooxygenase-2) or HIF1A (hypoxia-inducible factor 1-a)
462 independent manner (22). Also, a fibronectin fiber guided assay

Plastic and Reconstructive Surgery, Successful treatment with vascularized lymph node transfer and adipose stem cells in a mouse hindlimb lymphedema model

463 provides far stronger sprouting and guidance cues to endothelial cells.
464 VEGF-A, but not VEGF-C, stimulates the collective outgrowth of
465 lymphatic endothelial cells (LEC) (23) and Neuropilin-2 can mediate
466 lymphangiogenesis via an integrin α 9 β 1/FAK/Erk pathway but is
467 independent of VEGFC/VEGFR3 signaling in colorectal carcinoma
468 (24). These findings suggest that VEGF-C and VEGF-C/VEGFR3 are
469 not the only primary induction factors in lymphangiogenesis.
470 Lymphatic vessels are specifically immunoreactive to LYVE-1 and
471 the degree of augmentation with ADSCs is almost equal to that in
472 the presence or no presence of VLNTs.

473 In VLNT groups, B16 melanoma transplantation into the paw led to
474 all three animals when with ADSCs to die of tumor progression by
475 day 25. Gross lymph node metastasis and in-transit metastasis was
476 present in the flaps of all experimented animals with VLNT by day
477 28. As lymphatic drainage from murine B16 melanomas in syngeneic,
478 immune-competent C57Bl/6 mice is associated with LN enlargement
479 (25). In this experiment, function of lymphatic transport capacity
480 was tested in groups of VLNT plus / ADSCs minus or VLNT plus /

Plastic and Reconstructive Surgery, Successful treatment with vascularized lymph node transfer and adipose stem cells in a mouse hindlimb lymphedema model

481 ADSCs plus. In time course, all animals are dead by day 28 in VLNT
482 plus / ADSCs plus group. This would explain the VLNTs are able to
483 transport the lymphatic flow and more enhanced with existence of
484 ADSCs, because the rate of the lymph node metastases at day 21 and
485 more aggressive systemic effects by 28. There is no statistical
486 analysis in this specific experiment but all animals are dead in VLNT
487 plus / ADSCs plus group may lead to the enormous effects by both
488 VLNT and ADSCs, thus in clinical situation, it is highly cautious
489 when the “malignancy” exists.

490 Treatment model of secondary lymphedema by both ADSCs and
491 VLNTs was proposed through lymphangiogenesis and the decrease of
492 edema volumes through accelerated lymphatic drainage to the
493 venous systems.

494

Plastic and Reconstructive Surgery, Successful treatment with vascularized lymph node transfer and adipose stem cells in a mouse hindlimb lymphedema model

495 **Figure Legends**

496

497 **Figure 1**

498 Experimental design. X-ray radiation in the left inguinal region.

499

500 **Figure 2**

501 Anatomical features of vascularized lymph nodes. Arrow, the
502 superficial inferior epigastric artery; circle, subiliac lymph nodes.

503

504 **Figure 3**

505 Elevated vascularized flap with visible subiliac lymph nodes (top left).
506 VLNT to the ipsilateral 5-mm gap in the inguinal region.

507

508 **Figure 4**

509 The appearances of hind limbs at 14 days after surgery in Group 1
510 (control)

511

512 **Figure 5**

Plastic and Reconstructive Surgery, Successful treatment with vascularized lymph node transfer and adipose stem cells in a mouse hindlimb lymphedema model

513 The appearances of hind limbs at 14 days after surgery in Group 2
514 (VLNT alone)

515

516 Figure 6

517 The appearances of hind limbs at 14 days after surgery in Group 3
518 (ADSCs alone)

519

520 Figure 7

521 The appearances of hind limbs at 14 days after surgery in Group 4
522 (VLNT and ADSCs)

523

524 Figure 8

525 PDE images at 14 days after surgery in Group 1 (control).

526 The arrow points the transferred flap. The fluorescent imaging
527 representing lymphatic flow is not observed.

528

529 Figure 9

530 PDE images at 14 days after surgery in Group 2 (VLNT alone).

Plastic and Reconstructive Surgery, Successful treatment with vascularized lymph node transfer and adipose stem cells in a mouse hindlimb lymphedema model

531 The arrow points the transferred flap, the superficial inferior
532 epigastric vein was detected by ICG staining through the transferred
533 lymph nodes. Fluorescent imaging toward the proximal trunks was
534 not observed.

535

536 Figure 10

537 PDE images at 14 days after surgery in Group 3 (ADSCs alone).

538 The circle points small linear fluorescent imaging was observed in
539 the proximal region of the flap, which was supposed to restore

540 superficial collecting lymph vessels running along the ischiatic vein.

541 Staining was not observed within the flap as indicated by the arrow.

542

543 Figure 11

544 PDE images at 14 days after surgery in Group 4 (VLNT and ADSCs).

545 The arrow indicated the flap the transferred subiliac lymph nodes

546 was stained immediately. The lymph node flap shunted lymphatic

547 fluid from the recipient bed, via lymph nodes, into the flap's pedicle

Plastic and Reconstructive Surgery, Successful treatment with vascularized lymph node transfer and adipose stem cells in a mouse hindlimb lymphedema model

548 vein. The circle represents linear fluorescent imaging was also
549 observed in the proximal region of the flap as in Group 3

550

551

552 Figure 12

553 Hind paw volume measurement. In all groups, hind limb
554 lymphedema was observed at 2 days after surgery. A significantly
555 lower paw volume was detected in Group 4 compared with other
556 groups at 14 days after surgery ($p<0.05$).

557

558 Figure 13

559 The ratio of hind paw volume improvement. The percentage of
560 improved difference was significantly greater in Group 4 compared
561 with other groups ($p<0.05$).

562

563 Figure 14

564 The percentage of deterioration difference was significantly lower in
565 Group 4 compared with other groups ($p<0.05$).

Plastic and Reconstructive Surgery, Successful treatment with vascularized lymph node transfer and adipose stem cells in a mouse hindlimb lymphedema model

566

567 Figure 15

568 The number of lymphatic vessels with LYVE-1 immunoreactivity.

569 The numbers of lymphatic vessels in Group 3 and Group4 were

570 significantly increased compared with those in Group 1 and Group 2

571 ($p < 0.05$).

572

573 Figure 16

574 Representative photographs of the hind limbs in VLNT plus / ADSCs

575 minus group. 28 days after tumor cell transplantation, gross

576 metastasis to the lymph nodes and in-transit metastasis in their

577 flaps were seen.

578

579 Figure 17

580 Representative photographs of the hind limbs in VLNT plus / ADSCs

581 plus group. 21 days after tumor cell transplantation, there were

582 metastatic skin tumors on the trunks. The arrow indicates

583 transferred lymph nodes. The circle indicates metastatic skin tumor.

Plastic and Reconstructive Surgery, Successful treatment with vascularized lymph node transfer and adipose stem cells in a mouse hindlimb lymphedema model

584

585 Figure 18

586 B16 Melanoma cells caused transferred lymph node metastases in
587 both VLNT plus / ADSCs minus and VLNT plus / ADSCs plus groups
588 and multiple skin metastases in VLNT plus / ADSCs plus group.

589 Melanoma cells were immunoreactive to Melan-A.

590 Transferred subiliac lymph node at high magnification in VLNT plus
591 / ADSCs minus group.

592

593 Figure 19

594 B16 Melanoma cells caused transferred lymph node metastases in
595 both VLNT plus / ADSCs minus and VLNT plus / ADSCs plus groups
596 and multiple skin metastases in VLNT plus / ADSCs plus group.

597 Melanoma cells were immunoreactive to Melan-A.

598 The metastatic skin tumor at high magnification in VLNT plus /
599 ADSCs plus group.

600

601 Table 1

Plastic and Reconstructive Surgery, Successful treatment with vascularized lymph node transfer and adipose stem cells in a mouse hindlimb lymphedema model

602 Study design

603

604

605 References

606

607 1. Sheila N. Blumberg, Todd Berland, Caron Rockman, Firas Mussa,
608 Allison Brooks, Neal Cayne and Thomas Maldonado. Pneumatic
609 Compression Improves Quality of Life in Patients with Lower-
610 Extremity Lymphedema. *Ann Vasc Surg* 2016;30:40-44.

611

612 2. Yamamoto T, Yamamoto N, Doi K, et al. Indocyanine
613 greenenhanced lymphography for upper extremity lymphedema:
614 a novel severity staging system using dermal backflow patterns.
615 *Plastic and Reconstructive Surgery* 2011; 128: 941-47.

616

617 3. Koshima I, Narushima M, Yamamoto Y, Mihara M, Iida T.
618 Recent advancement on surgical treatments for lymphedema.
619 *Ann Vasc Dis* 2012;5:409–415.

620

621 4. Becker C, Assouad J, Riquet M, Hidden G. Postmastectomy
622 lymphedema: Long-term results following microsurgical lymph

Plastic and Reconstructive Surgery, Successful treatment with vascularized lymph node transfer and adipose stem cells in a mouse hindlimb lymphedema model

623 node transplantation. *Ann Surg* 2006; 243: 313–315.

624

625 5. Cheng MH, Chen SC, Henry SL, et al. Vascularized groin lymph
626 node flap transfer for postmastectomy upper limb lymphedema:
627 flap anatomy, recipient sites, and outcomes. *Plast Reconstr Surg*
628 2013; 131:1286-98.

629

630 6. Saaristo AM, Niemi TS, Viitanen TP, et al. Microvascular breast
631 reconstruction and lymph node transfer for postmastectomy
632 lymphedema patients. *Ann Surg* 2012; 255: 468-73.

633

634 7. Cheng MH, Huang JJ, Nguyen DH, et al. A novel approach to the
635 treatment of lower extremity lymphedema by transferring a
636 vascularized submental lymph node flap to the ankle. *Gynecol*
637 *Oncol* 2012; 126: 93-8.45.

638

639 8. Jeltsch M, Kaipainen A, Joukov V et al. Hyperplasia of lymphatic
640 vessels in VEGF-C transgenic mice. *Science* 1997;276:1423–1425.

Plastic and Reconstructive Surgery, Successful treatment with vascularized lymph node transfer and adipose stem cells in a mouse hindlimb lymphedema model

641

642 9. Makinen T, Veikkola T, Mustjoki S et al. Isolated lymphatic
643 endothelial cells transduce growth, survival and migratory
644 signals via the VEGF-C/D receptor VEGFR-3. *EMBO J*
645 2001;20:4762–477.

646

647 10. Takeda K, Sowa Y, Nishino K, Itoh K, Fukushiki S.
648 Adiposederived stem cells promote proliferation, migration, and
649 tube formation of lymphatic endothelial cells in vitro by secreting
650 lymphangiogenic factors. *Ann. Plast Surg* 2014;74:728–736.

651

652 11. Yoshida S, Hamuy R, Hamada Y, Yoshimoto H, Hirano A, Akita
653 S. Adipose-derived stem cell transplantation for therapeutic
654 lymphangiogenesis in a mouse secondary lymphedema model.
655 *Regen Med* 2015;10:549-62.

656

657 12. Hwang JH, Kim IG, Lee JY et al. Therapeutic
658 lymphangiogenesis using stem cell and VEGF-C hydrogel.

Plastic and Reconstructive Surgery, Successful treatment with vascularized lymph node transfer and adipose stem cells in a mouse hindlimb lymphedema model

659 Biomaterials 2011;32:4415–4423.

660

661 13. DiSipio T, Rye S, Newman B, Hayes S. Incidence of unilateral
662 arm lymphedema after breast cancer: a systematic review and
663 meta-analysis. *Lancet Oncol* 2013;14:500–515.

664

665 14. Warren LE, Miller CL, Horick N et al. The impact of radiation
666 therapy on the risk of lymphedema after treatment for breast
667 cancer: a prospective cohort study. *Int J Radiat Oncol Biol Phys*
668 2014;88:565–571.

669

670 15. Avraham T, Daluvoy S, Zampell J et al. Blockage of
671 transforming growth factor- β 1 accelerates lymphatic
672 regeneration during wound repair. *Am J Pathol* 2010;177: 3202–
673 3214.

674

675 16. Choi I, Lee S, Kyoung Chung H et al. 9-cis retinoic acid
676 promotes lymphangiogenesis and enhances lymphatic vessel

Plastic and Reconstructive Surgery, Successful treatment with vascularized lymph node transfer and adipose stem cells in a mouse hindlimb lymphedema model

677 regeneration: therapeutic implication of 9-cis retinoic acid for
678 secondary lymphedema. *Circulation* 2012;125:872–82.

679

680 17. Tammela T, Saaristo A, Holopainen T et al. Therapeutic
681 differentiation and maturation of lymphatic vessels after lymph
682 node dissection and transplantation. *Nat Med* 2007;13:1458–1466.

683

684 18. Festing MF, Altman DG. Guidelines for the design and
685 statistical analysis of experiments using laboratory animals.

686 *ILAR J.* 2002;43:244-58

687

688 19. Festing MF. Design and statistical methods in studies using
689 animal models of development. *ILAR J.* 2006;47:5-14

690

691 20. Sakuta T, Morita Y, Satoh M, Fox DA, Kashihara N.

692 Involvement of the renin-angiotensin system in the development

693 of vascular damage in a rat model of arthritis: effect of

694 angiotensin receptor blockers. *Arthritis Rheum* 2010;62:1319-

695 1328.

Plastic and Reconstructive Surgery, Successful treatment with vascularized lymph node transfer and adipose stem cells in a mouse hindlimb lymphedema model

696

697 21. Shioya R, Furukawa H, Murao N, Hayashi T, Oyama A,
698 Funayama E, Yamamoto Y, Saito N. Prevention of
699 Lymphedematous Change in the Mouse Hindlimb by
700 Nonvascularized Lymph Node Transplantation. *Ann Plast Surg.*
701 2015 Feb 7. Epub ahead of print

702

703 22. Larrieu-Lahargue F, Welm AL, Bouche-careilh M, Alitalo K, Li
704 DY, Bikfalvi A, Auguste P. Blocking Fibroblast Growth Factor
705 receptor signaling inhibits tumor growth, lymphangiogenesis,
706 and metastasis. *PLoS One* 2012;7:e39540.

707

708 23. Mitsi M, Schulz MM, Gousopoulos E, Ochsenbein AM, Detmar
709 M, Vogel V. Walking the Line: A Fibronectin Fiber-Guided Assay
710 to Probe Early Steps of (Lymph)angiogenesis. *PLoS One*
711 2015;10:e0145210.

712

713 24. Ou JJ, Wei X, Peng Y, Zha L, Zhou RB, Shi H, Zhou Q, Liang

Plastic and Reconstructive Surgery, Successful treatment with vascularized lymph node transfer and adipose stem cells in a mouse hindlimb lymphedema model

- 714 HJ. Neuropilin-2 mediates lymphangiogenesis of colorectal
715 carcinoma via a VEGFC/VEGFR3 independent signaling. *Cancer*
716 *Lett* 2015;358:200-209.
- 717
- 718 25. Rohner NA, McClain J, Tuell SL, Warner A, Smith B, Yun Y,
719 Mohan A, Sushnitha M, Thomas SN. Lymph node biophysical
720 remodeling is associated with melanoma lymphatic drainage.
721 *FASEB J.* 2015;29:4512-22.

Figure1

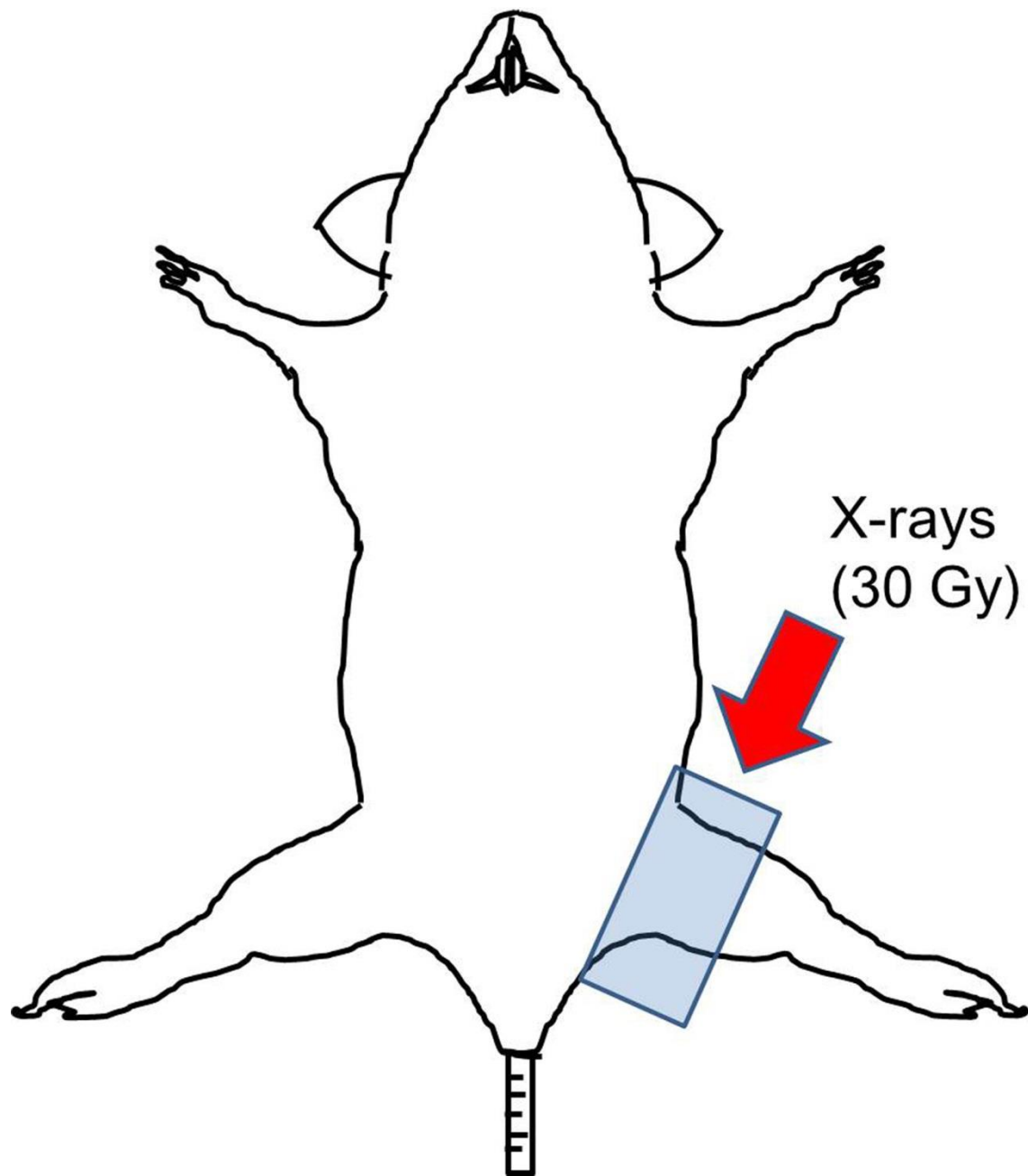


Figure 2

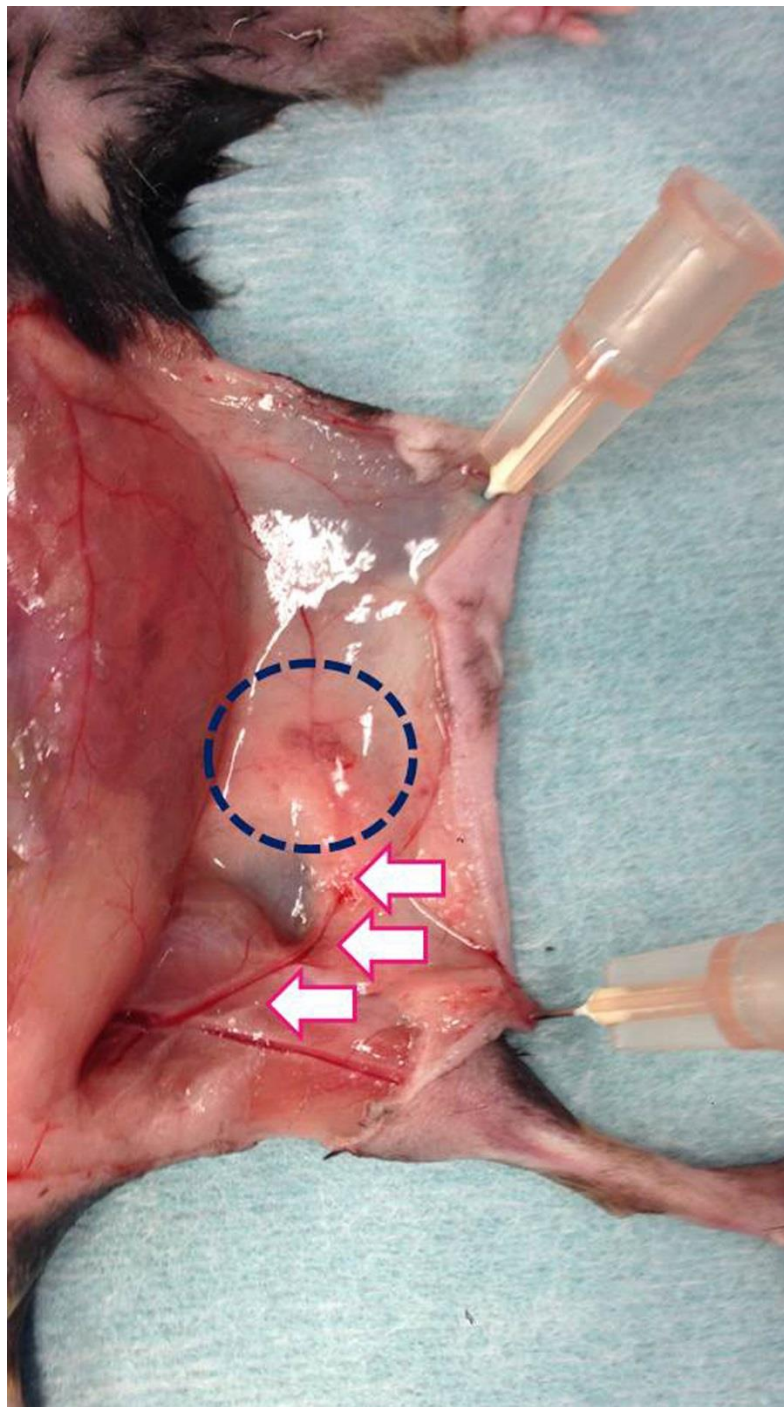


Figure3

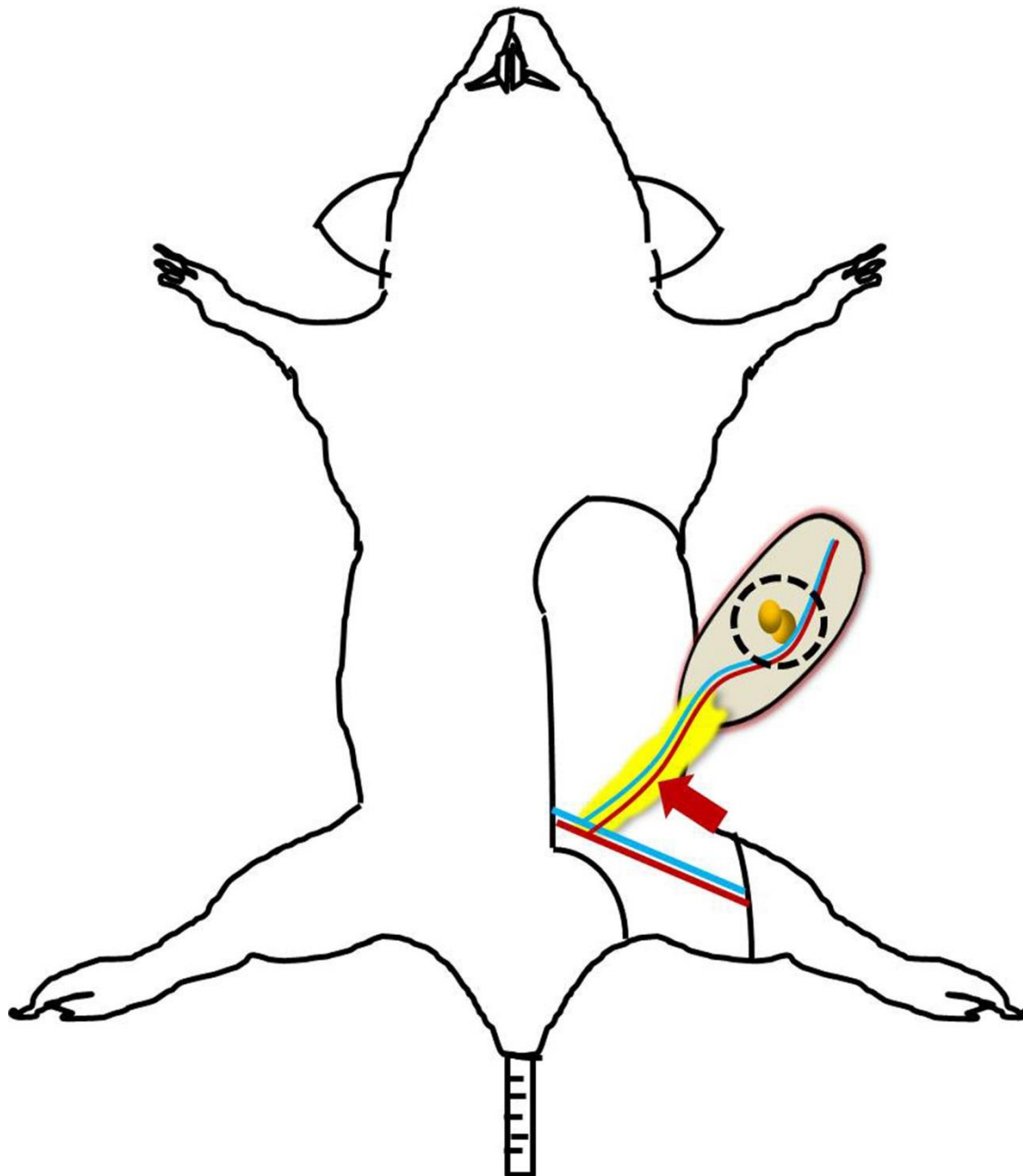


Figure4



Figure5



Figure6



Figure7



Figure8

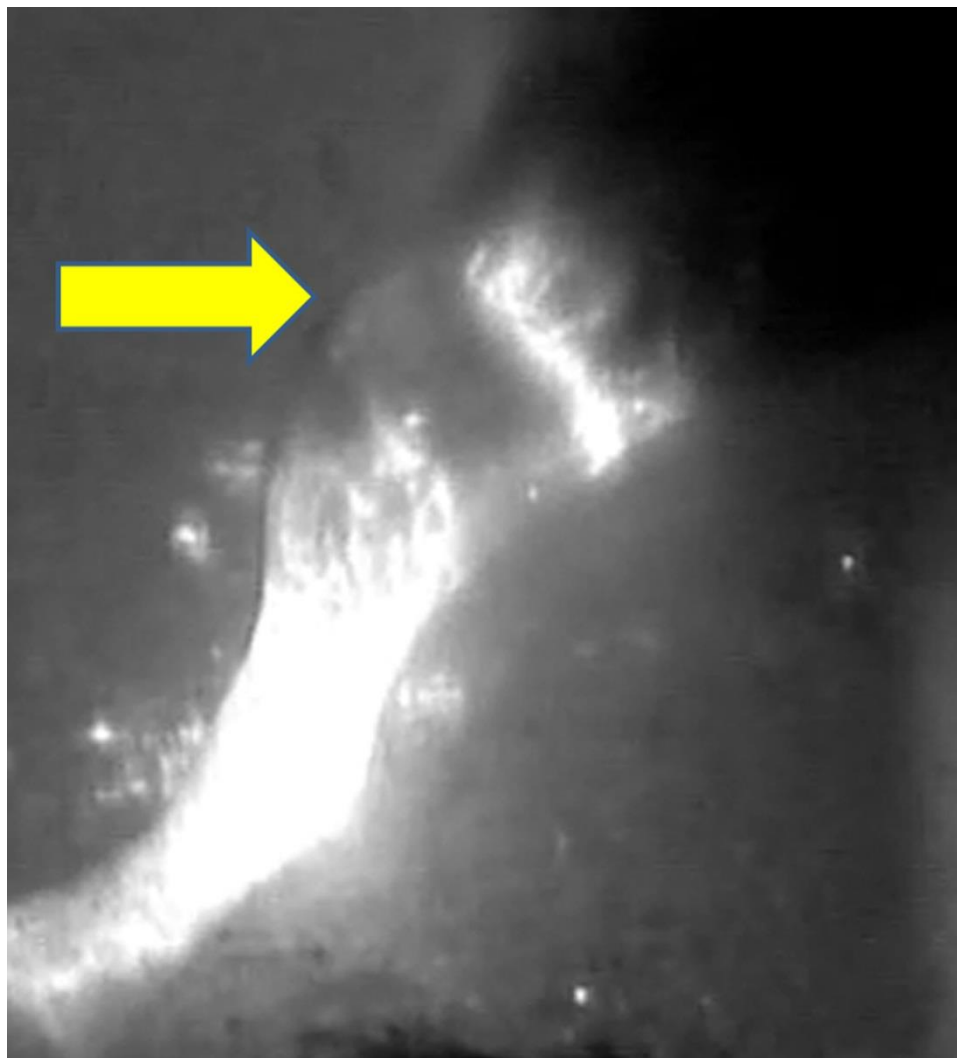


Figure9



Figure10

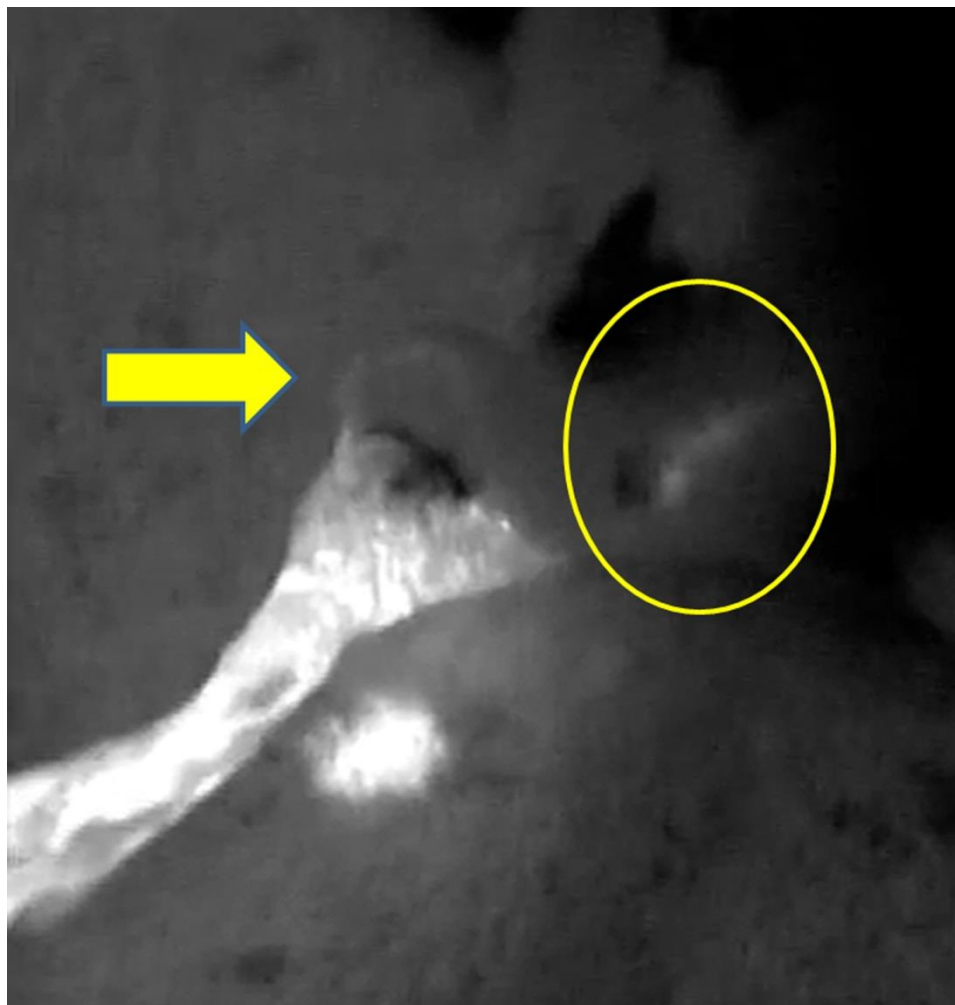


Figure11



Figure12

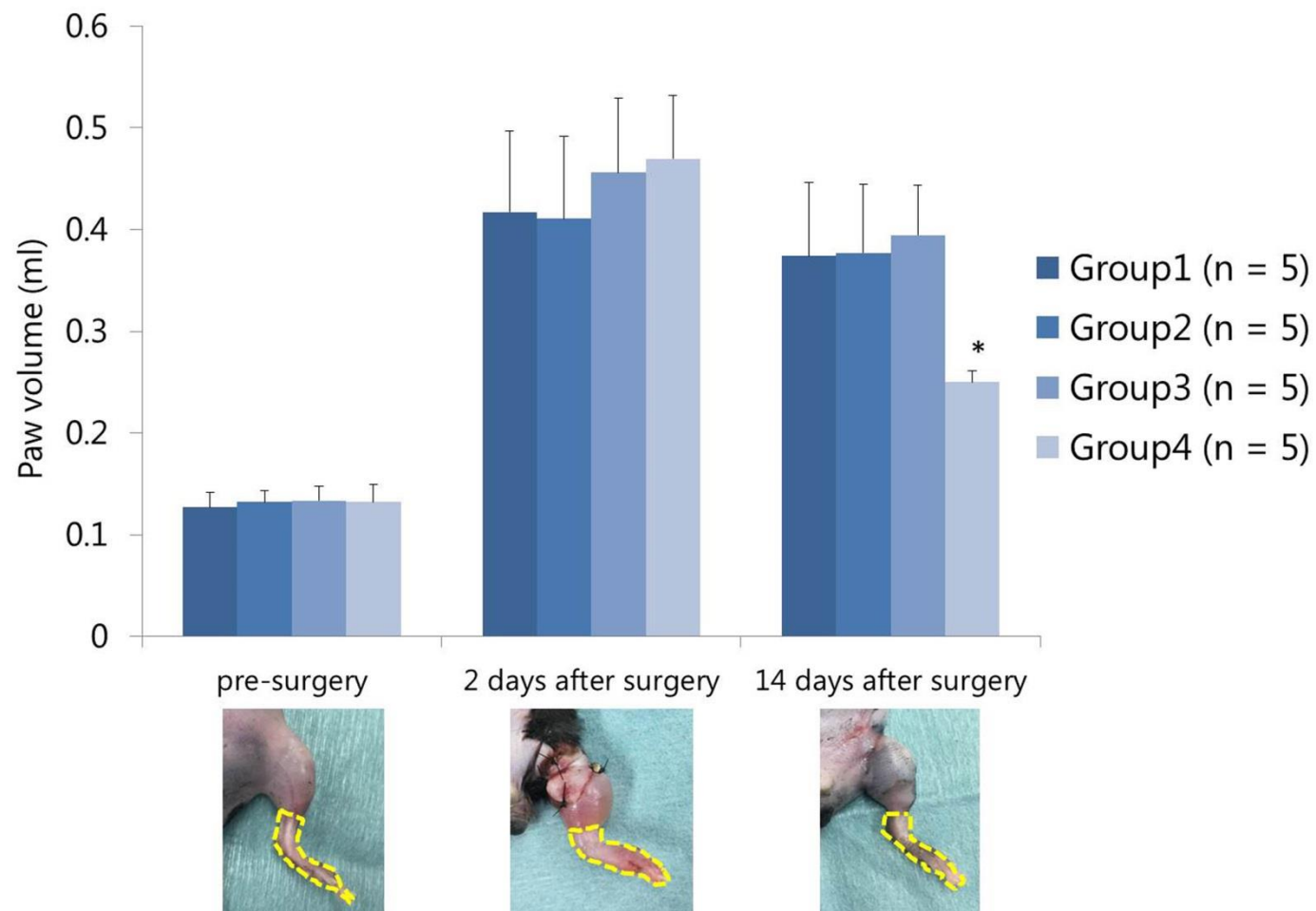


Figure13

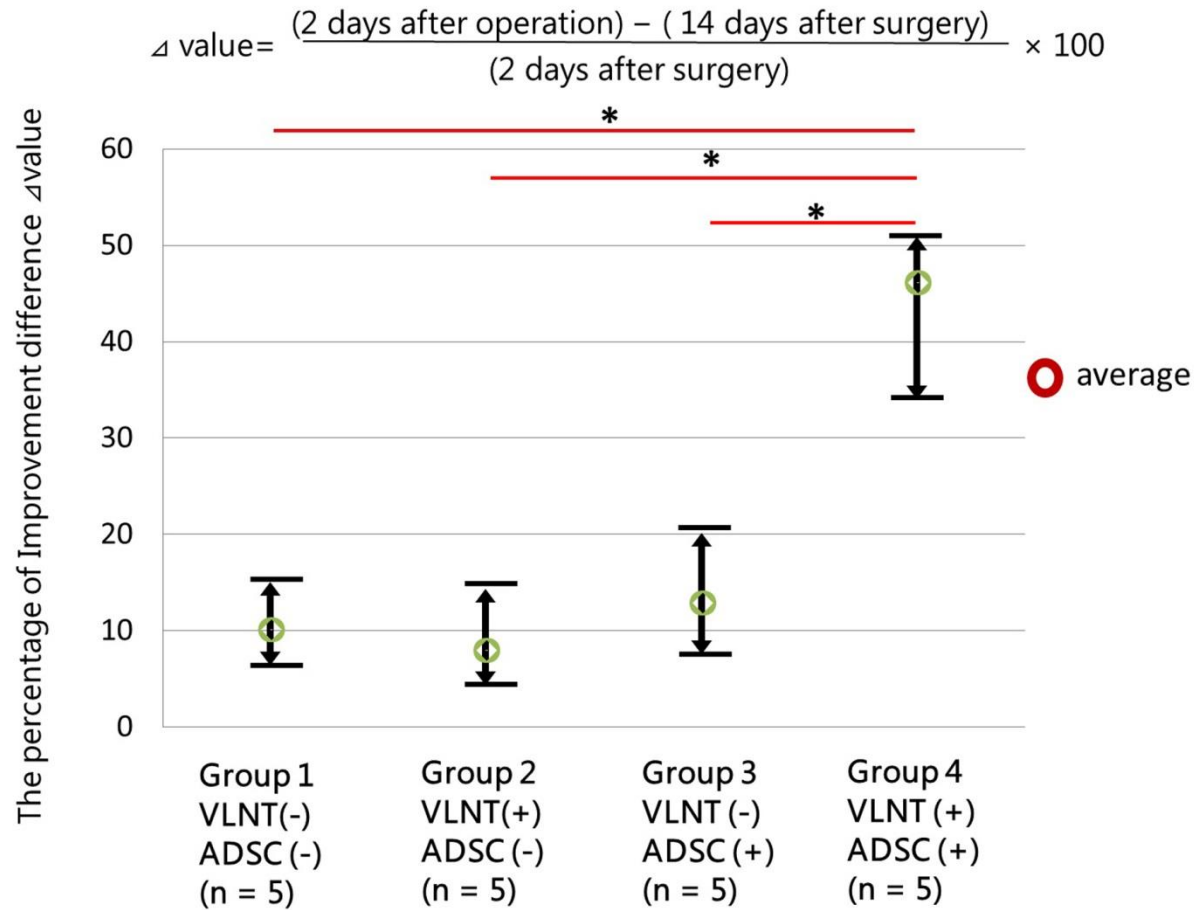


Figure14

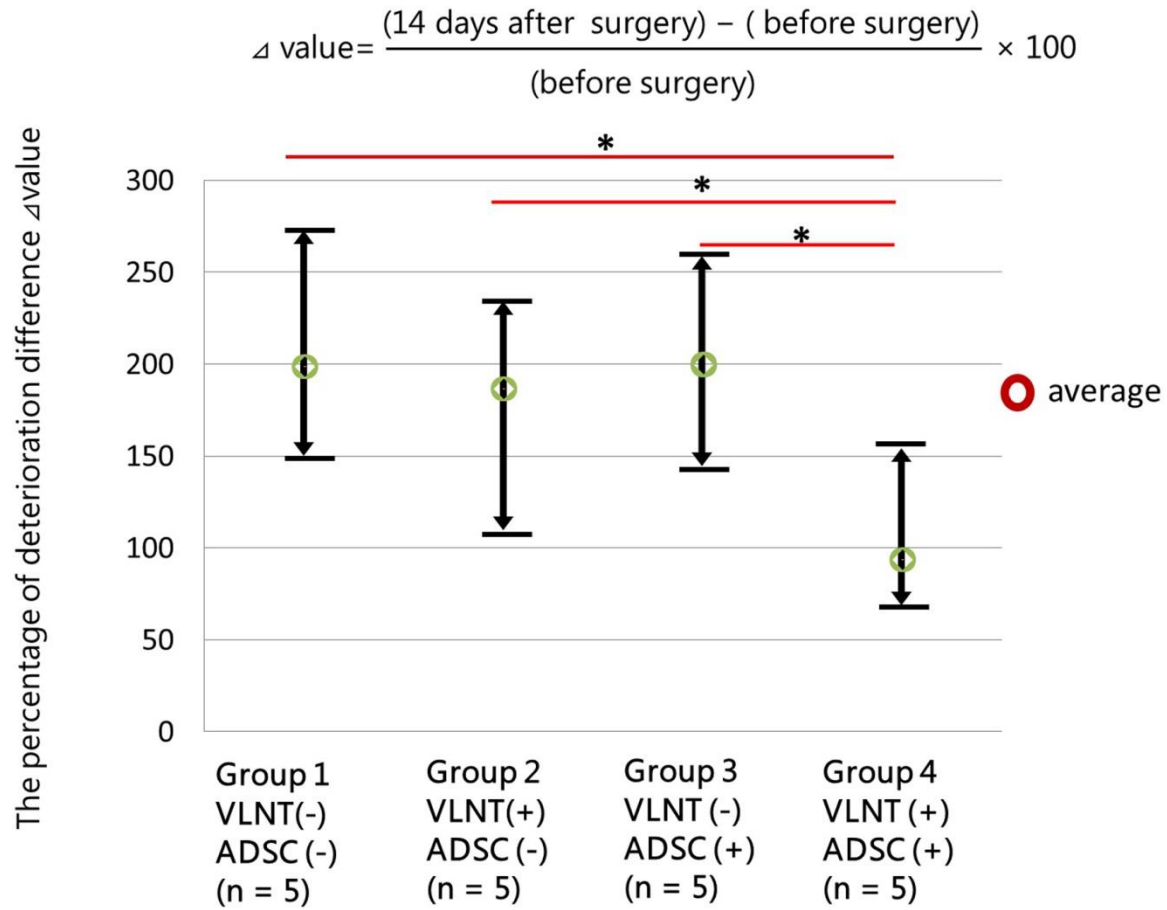


Figure15

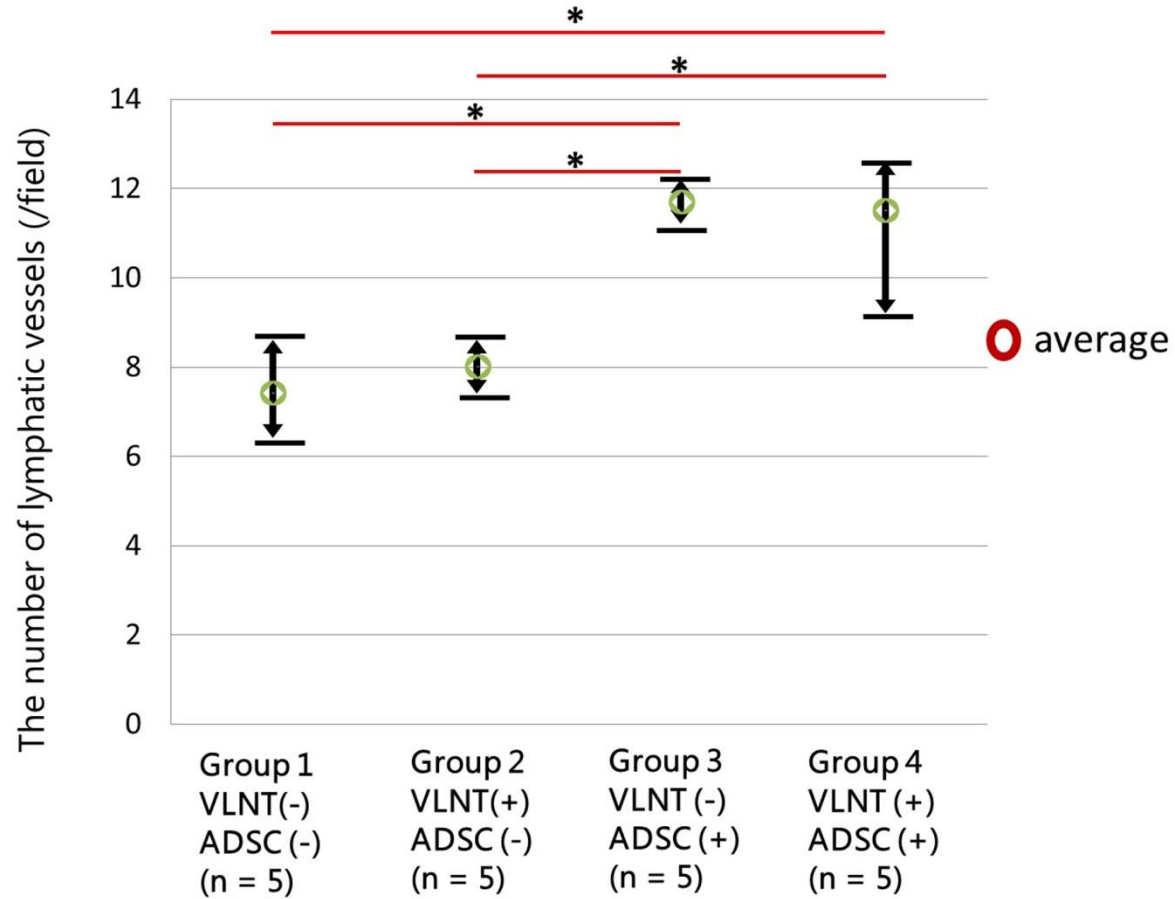


Figure16



Figure17

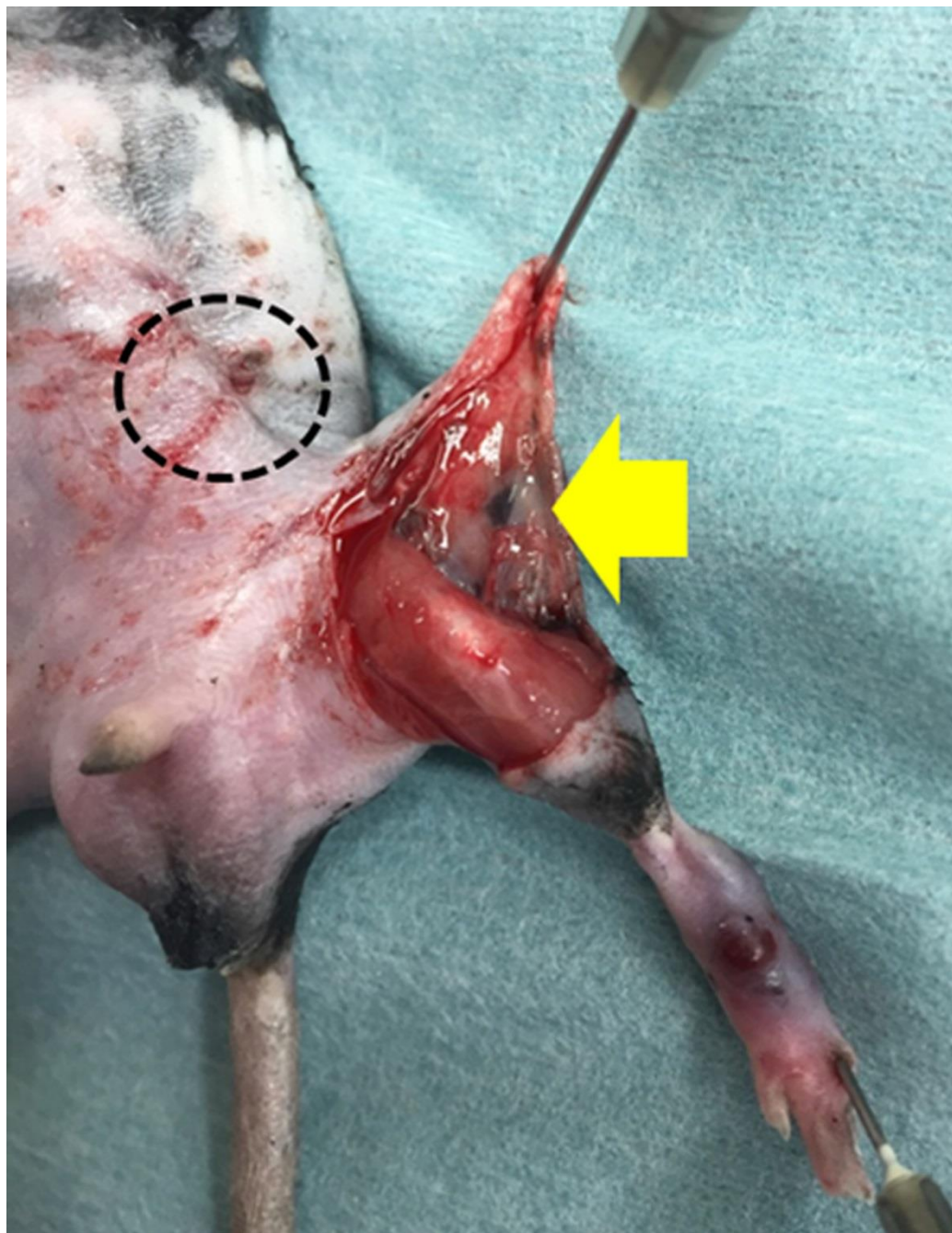


Figure18

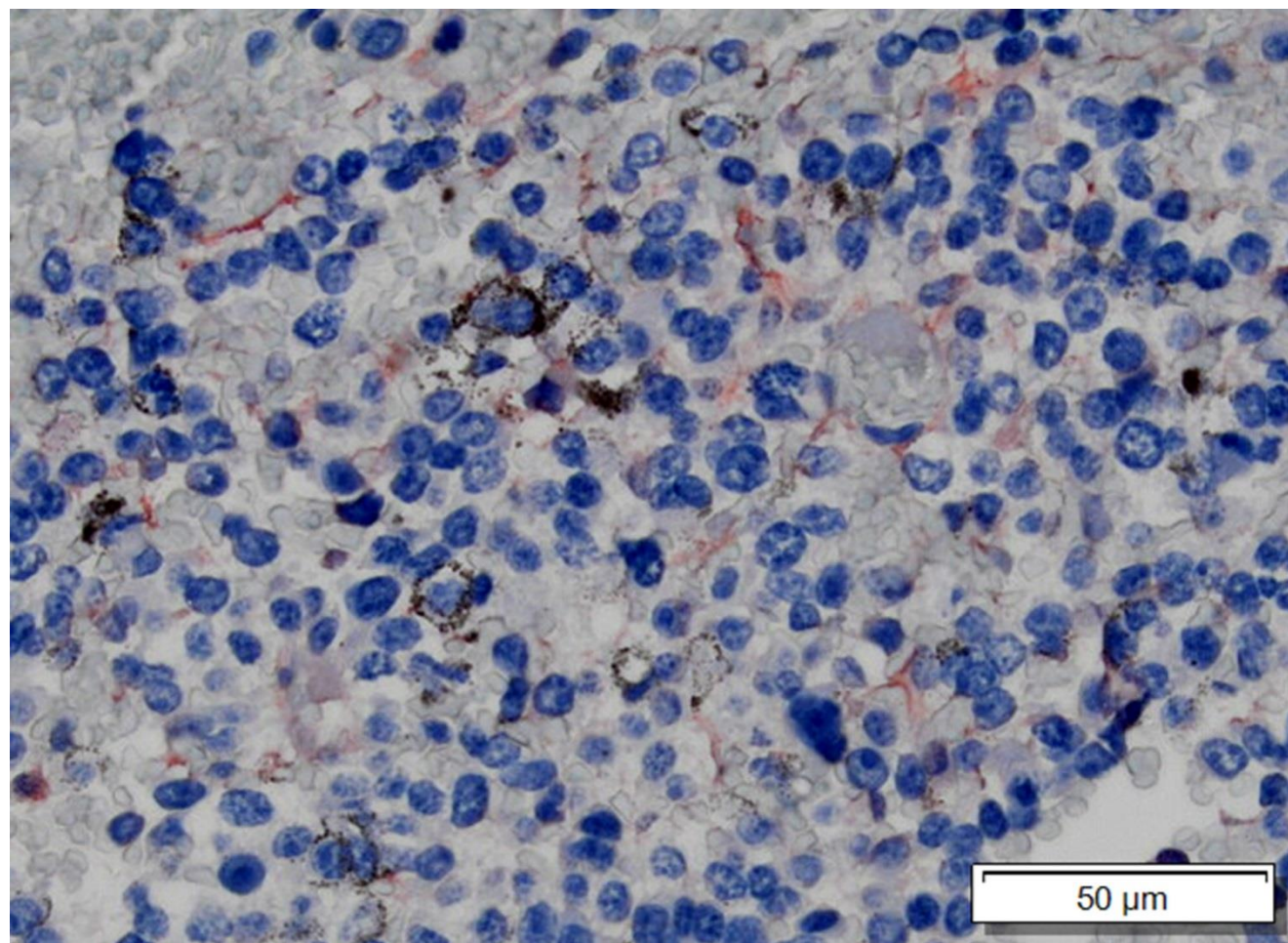


Figure19

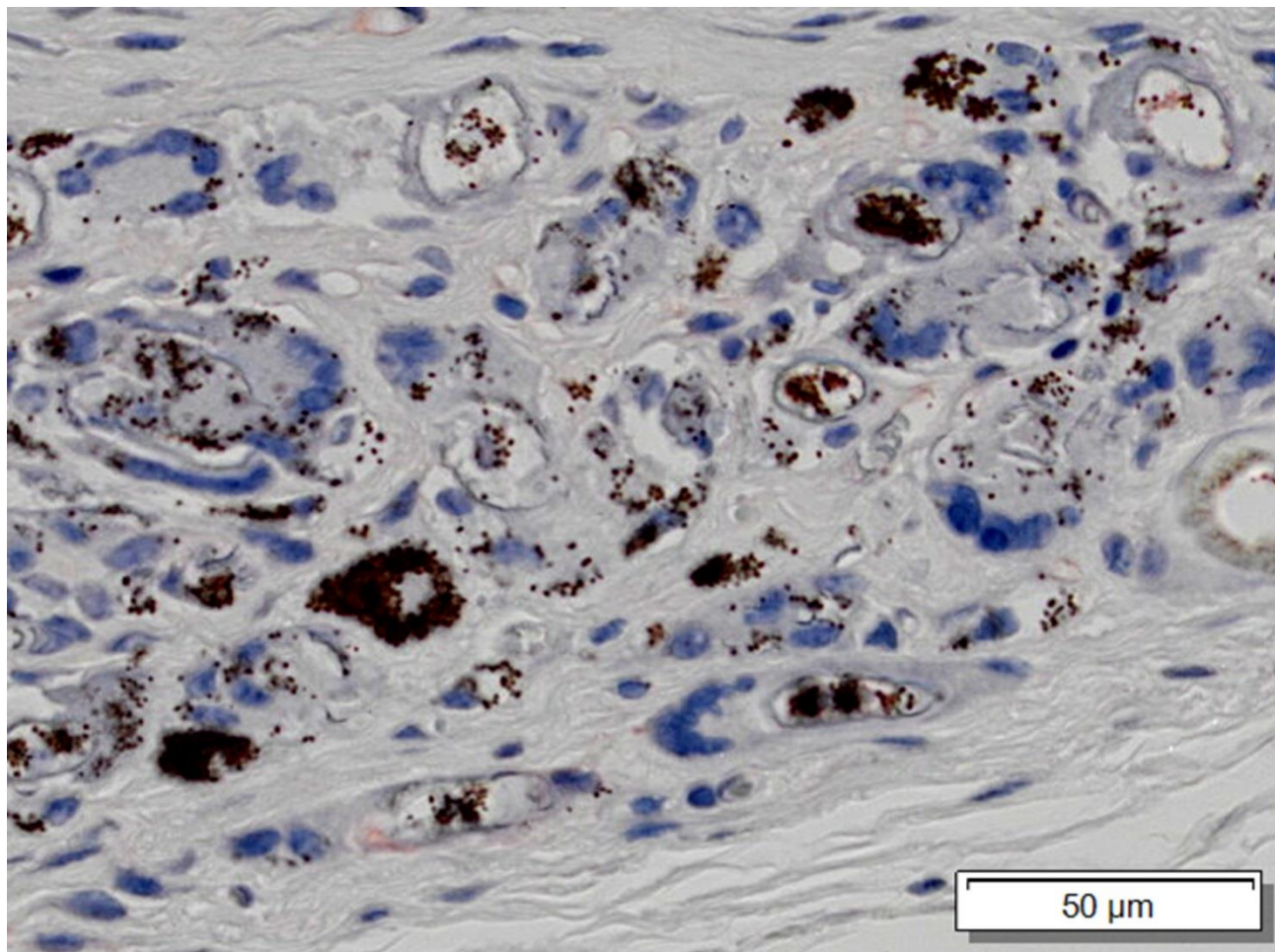


Table 1

